Periodic Heterogeneity-Driven Resonance Amplification in Density Fingering

D. Horváth, S. Tóth, and Á. Tóth

Department of Physical Chemistry, University of Szeged, P.O. Box 105, Szeged, H-6701, Hungary

(Received 23 June 2006; published 6 November 2006)

Periodic heterogeneity is introduced in experiments with thin solution layers where downward propagating planar autocatalytic fronts are hydrodynamically unstable and cellular patterns develop. The evolution of fingers is greatly affected by the spatial heterogeneity when the wave number associated with it falls in the vicinity of the most unstable mode of the reference system with uniform thickness. The imposed heterogeneity will drive the instability by amplifying the modes with the matching wave numbers as indicated by the experimentally constructed dispersion curves.

DOI: 10.1103/PhysRevLett.97.194501 PACS numbers: 47.70.Fw, 47.20.Bp, 47.55.P−, 82.40.Ck

In distributed systems chemical reactions with a positive feedback exhibit nontrivial concentration profiles as propagating fronts, rotating spirals, and stationary Turing patterns [1]. These spatiotemporal patterns resulting from the coupling of diffusion with nonlinear chemical kinetics are greatly affected by spatial inhomogeneities [2] or geometrical constraints [3]. Novel behavior may be observed when the interaction between the intrinsic length scale of the homogeneous system and that of the spatial perturbation leads to spatial resonance [4]. In these chemical systems it is a challenge to observe mode selection by resonance amplification similarly to acoustics. We address this issue in a reaction where the resultant convection is the important transport process, which is even more abundant in natural systems.

Convective instability arising along reactive interfaces is of recent interest in hydrodynamics [1,5,6]. Buoyant forces under gravity will distort the geometry of the planar interface when a solution with higher density is layered on top of another with lower density. If the two solutions comprise the reactant and the product mixtures of an autocatalytic reaction, the chemical reaction occurring at a significant rate only along the interface may maintain a constant density difference between the two parts [7–11]. The system can then be viewed in hydrodynamics as a pair of miscible fluids but with a diffusional layer of constant width between them as a result of the autocatalytic chemical reaction. Systematic studies of these hydrodynamically unstable reaction fronts exhibiting density fingering have been carried out in Hele-Shaw cells [12,13], where the fluid flow in most cases may be considered two dimensional because of the very thin liquid layer formed in the vessel [14]. Theoretical studies have also applied Darcy's law for fluid dynamics [15,16], hence approximating the thin layer of solution to a porous medium. The instability associated with fluid motion in porous media itself deserves attention in conjunction with various chemical applications. In natural materials pore size has a certain distribution forming a spatially heterogeneous medium. A theoretical work on viscous fingering [17] has pointed out the importance of the imposed wavelength in a periodically heterogeneous porous medium. In our experimental system, heterogeneity also refers to the spatially varying permeability which is created by constructing a Hele-Shaw cell with nonuniform gap width. Our goal is to investigate the interaction between the imposed heterogeneity and the hydrodynamic instability present in the uniform cell. To our best knowledge this is the first experimental study where a thin layer of reactive fluid exhibiting density fingering is placed in a nonuniform Hele-Shaw cell.

For the test reaction, we have selected the chlorite-tetrathionate reaction [18], which exhibits a variety of reaction-diffusion patterns from lateral instability in closed systems, where the autocatalyst is bound to an immobile species [19,20], to oscillations and excitability in open systems based on long range activation [21,22]. The characteristics of the hydrodynamic instability accompanying chemical fronts of the reaction under gravity in thin solution layers have also been studied thoroughly both experimentally [13,23,24] and theoretically [25–27]. The fresh reactant mixture has lower density than that of the product solution, therefore in thin solutions only upward propagating planar fronts retain their geometry. Downward propagating planar fronts, on the other hand, are hydrodynamically unstable and density fingering will lead to the formation of cellular patterns, where the reaction front profile consists of curved segments, called cells, joined in sharp cusps.

In our experiments, the reactant mixture [28] is poured into a vertically positioned Hele-Shaw cell of size 16 cm × 12 cm × 0.6 mm with 8 mm thick Plexiglas walls. The appropriate nonuniformity is introduced in the form of 0.1 mm deep vertical grooves in the inner walls of the cell as shown in Fig. 1. Several Hele-Shaw cells have been constructed with variations in the width and the spacing of the grooves (3–12 mm) in order to change the spatial scaling of the heterogeneity. Planar fronts are initiated electrochemically at the anode by applying a 3 V potential difference between a pair of thin Pt-wire electrodes (0.4 mm in diameter) positioned either at the top or at the bottom of the Hele-Shaw cell for 2–3 s. The front evolu-

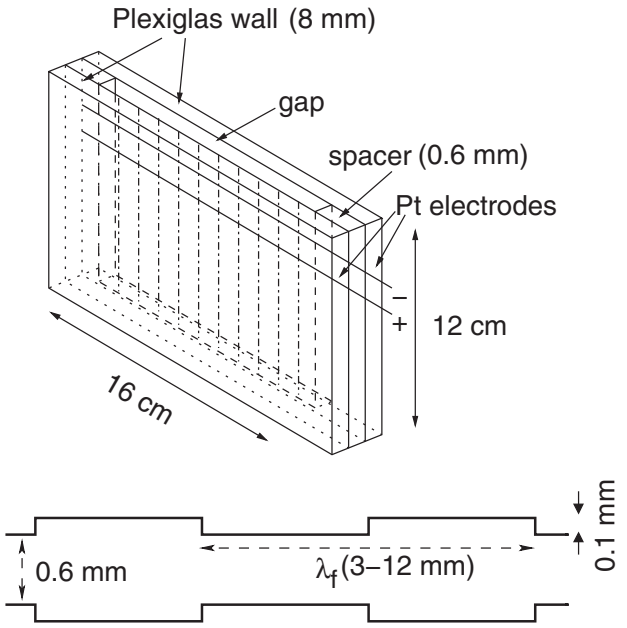

FIG. 1. Scheme of the Hele-Shaw cell (top), top view of a segment of the gap in the cell (bottom).

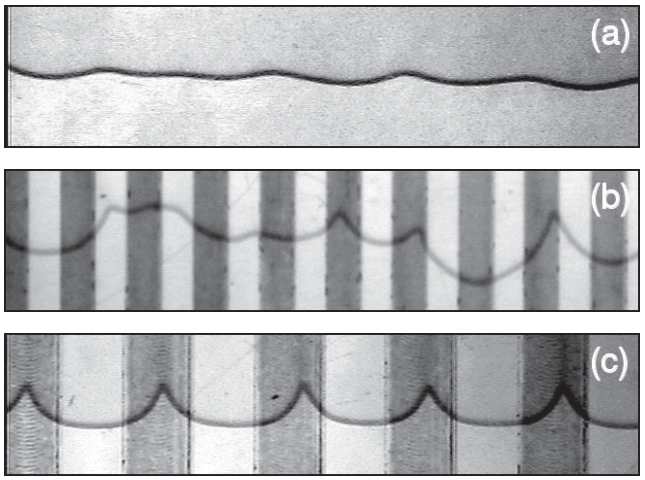

FIG. 2. Downward propagating fronts in a homogeneous (a) and heterogeneous Hele-Shaw cells with periodicity of $\lambda_f = 3$ mm (b) and $\lambda_f = 6$ mm (c) at 180 s. The darker vertical bars in (b) and (c) correspond to the location of grooves where the gap width is greater (0.8 mm). Field of view: 27.8 mm × 6.1 mm. The solution was prepared at a temperature of (25 ± 1) °C with reagent-grade chemicals using the following composition: $[K_2S_4O_6] = 2.5$ mM, $[NaClO_2] = 10$ mM, $[NaOH] = 1$ mM, and Congored indicator in 0.4 mg/cm^3 concentration.

tion is monitored in the central region of the reaction vessel by a monochrome CCD camera through a broadband filter with a maximum transmittance at 590 nm and digitized in 0.4–1 s intervals by an MVDelta imaging board. A one-dimensional Fourier transformation is applied on the front profiles with a Hann window to determine the Fourier amplitudes, which exponentially grow or decay in the early stages of the front evolution. The growth rates are hence calculated for the first 30 Fourier modes from the slopes of the initial linear time evolution of the logarithm of the Fourier amplitudes. Each dispersion curve is the result of averaging at least six experiments. The spatial scaling of the nonuniformity, the thickness of the Hele-Shaw cell and the chemical composition of the solutions have been varied systematically to find the appropriate conditions for interaction between the density difference driven convective instability and the periodic modulation of gap width in the direction of the reacting interface.

In the present study, the hydrodynamical stability of the upward propagating planar reaction fronts remains undisturbed upon the introduction of the nonuniform gap width with 0.1 mm deep square grooves. In the case of downward propagating fronts, the periodic heterogeneity with $\lambda_f = 3$ mm only mildly increases the growth rate of finger evolution. It has no effect on the average size of fingers with respect to that observed in a uniform Hele-Shaw cell as shown in Fig. 2(a) and 2(b). There is, however, a significant change in the behavior when the variation of gap width has a wavelength of $\lambda_f = 6$ mm: the initial fingers align themselves along the vertical grooves. Figure 2(c) illustrates that the leading segments of fingers evolve in the thinner regions, while the sharp cusps joining the neighboring fingers appear in the thicker channels. Furthermore, the initial fingers grow considerably faster reaching an approximately constant amplitude and wavelength (see Fig. 3).

The initial pattern formation may be best characterized quantitatively by constructing the dispersion curves. In a homogeneous Hele-Shaw cell, considered a reference system in this work, a parabola from the origin (the solid line in Fig. 4) describes the observed behavior. The most unstable mode at a wave number of $k_m = 1.14 \pm 0.02$ mm^{-1}, i.e., a wavelength of $\lambda_m = 5.5 \pm 0.1$ mm, has a growth rate $\omega_m = 0.021 \pm 0.001$ s^{-1}. The characteristics of the dispersion curve do not change when the periodic nonuniformity is applied with $\lambda_f = 3$ mm as expected from the visual observation of Fig. 2(b). The general increase in the growth rates may be contributed to the increase in the average gap width [23]. The striking change in the dispersion curve occurs when the spatial heterogeneity has $\lambda_f = 6$ mm corresponding to $k = 1.05$ mm^{-1}; strong amplification develops in the appropriate modes, underlying the fast appearance of uniform fingers shown in Fig. 3(b). Doubling the wavelength of the spatial modulation of gap width, by carrying out the experiments in a Hele-Shaw cell with twice as wide grooves and spacing between them, results in smaller amplification at two wave numbers: one that corresponds to the wavelength associated with the vertical grooves and the other is its first overtone. The latter yields the fastest growing mode with $\omega_m = 0.044 \pm 0.001$ s^{-1} because it falls in the vicinity of the most unstable mode observed in the uniform Hele-Shaw cell.

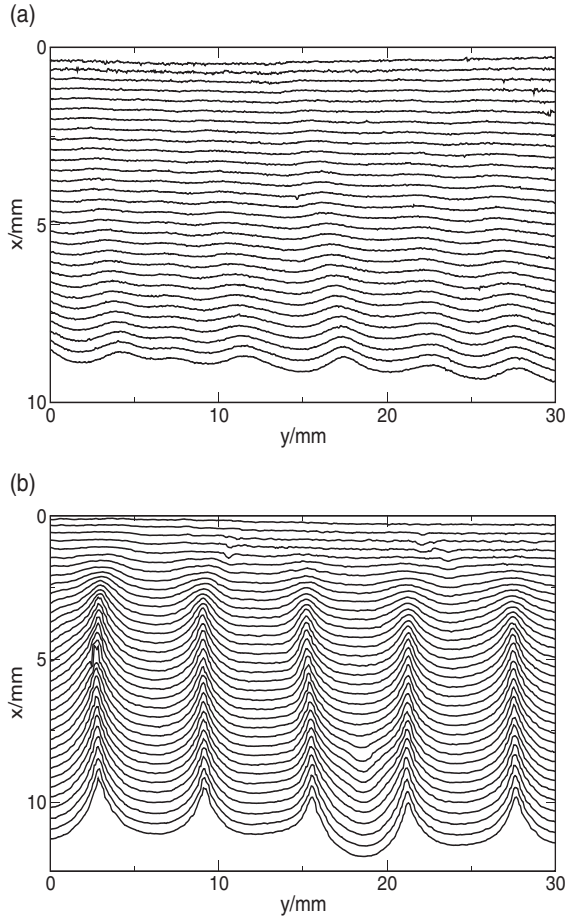

FIG. 3. Front evolution for a reactive interface in the uniform reference system of Fig. 2(a) (top) and in the heterogeneous Hele-Shaw cell of Fig. 2(c) (bottom) at time intervals $\Delta t = 6$ s.

Figure 4 also clearly illustrates that upward propagating fronts under the periodic spatial heterogeneity remain stable as all of the growth rates are negative; hence initial perturbations of the planar structure decay in time.

The results suggest that patterns developing in the homogeneous Hele-Shaw cell with the fastest growing mode at $k_m \approx 1$ mm^{-1} would experience resonance amplification when the spatial heterogeneity has the same wave number. Therefore the concentration of chemicals have been varied to design another system with a dispersion relation where the maximal growth rate satisfies the requirement. The increase of both the initial reactant concentrations and the removal of the autocatalyst gives rise to patterns with the most unstable mode at $k = 1.24 \pm 0.03$ mm^{-1} and $\omega = 0.023 \pm 0.002$ s^{-1} in a homogeneous Hele-Shaw cell as shown in Fig. 5. Using the periodic spatial heterogeneity of $\lambda_f = 6$ mm, we have carried out experiments and have found that indeed a threefold amplification exists at the appropriate wave number.

We have illustrated that spatial periodic heterogeneity can lead to resonance amplification of modes with the corresponding wavelengths. The amplification is at maximum when the wave number of the imposed nonuniformity

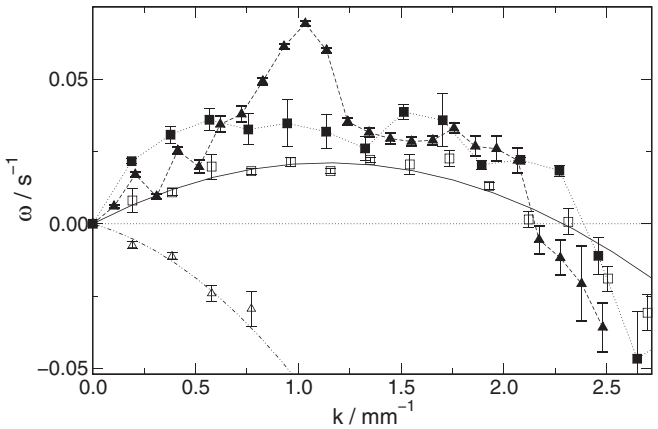

FIG. 4. Dispersion curves with growth rate ω versus wave number k for downward propagating fronts in a homogeneous Hele-Shaw cell (□), in nonuniform vessels with $\lambda_f = 3$ mm (■) and $\lambda_f = 6$ mm (▲). Also shown the dispersion curve for stable upward propagating fronts in a nonuniform Hele-Shaw cell with $\lambda_f = 6$ mm (△). The solid line and the dash-dotted line correspond to the appropriate fitted parabolas. The dashed and dotted lines are drawn to aid the eyes.

matches that of the most unstable mode in the uniform Hele-Shaw cell. However, no change in the characteristics of the dispersion curve occurs when it is around the marginal wave number or beyond. Systems with similar dispersion relation yield resonance amplification under the same geometric constraints. Resonance amplification is known to arise in a number of different areas from earthquakes [29] to acoustics[30], but in chemical and biological systems temporal forcing is more common [31,32]. In our system a spatial modulation of a parameter interacts with the matching spatial mode determined by the physical

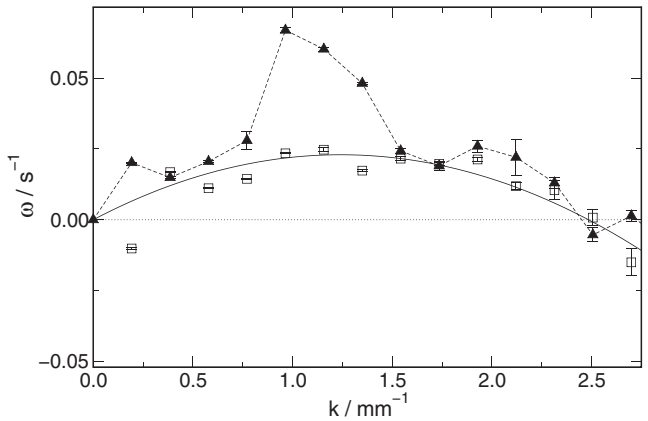

FIG. 5. Dispersion curves with growth rate ω versus wave number k for downward propagating fronts in a homogeneous Hele-Shaw cell (□) and in a heterogeneous vessel with $\lambda_f = 6$ mm periodic heterogeneity (▲). The solid line is a fitted parabola; the dashed line is drawn to aid the eyes. The solution composition: $[K_2S_4O_6] = 5.0$ mM, $[NaClO_2] = 20$ mM, $[NaOH] = 10$ mM, and Congored indicator in 0.4 mg/cm^3 concentration.

and chemical parameters of the fluid. The experiments represent the first step in investigating hydrodynamic pattern formation of reacting interfaces in porous media with spatially varying permeability.

The authors thank Professor A. De Wit and Dr. D. Lima for fruitful discussions. This work is financially supported by the Hungarian Scientific Research Fund (OTKA, No. T46010) and ESA (No. C98036).

*Electronic address: atoth@chem.u-szeged.hu

[1] I. R. Epstein and J. A. Pojman, *An Introduction to Nonlinear Dynamics: Oscillations, Waves, Patterns, and Chaos* (Oxford University Press, Oxford, United Kingdom, 1998).
[2] O. Steinbock, P. Kettunen, and K. Showalter, Science **269**, 1857 (1995).
[3] K. Agladze, J. P. Keener, S. C. Müller, and A. Panfilov, Science **264**, 1746 (1994).
[4] M. D. Graham, M. Bär, I. G. Kevrekidis, K. Asakura, J. Lauterbach, H.-H. Rotermund, and G. Ertl, Phys. Rev. E **52**, 76 (1995).
[5] M. C. Rogers and S. W. Morris, Phys. Rev. Lett. **95**, 024505 (2005).
[6] J. D'Hernoncourt, A. Zebib, and A. De Wit, Phys. Rev. Lett. **96**, 154501 (2006).
[7] I. Nagypál, Gy. Bazsa, and I. R. Epstein, J. Am. Chem. Soc. **108**, 3635 (1986).
[8] J. A. Pojman and I. R. Epstein, J. Phys. Chem. **94**, 4966 (1990).
[9] J. A. Pojman, I. R. Epstein, T. J. McManus, and K. Showalter, J. Phys. Chem. **95**, 1299 (1991).
[10] J. Masere, D. A. Vasquez, B. F. Edwards, J. W. Wilder, and K. Showalter, J. Phys. Chem. **98**, 6505 (1994).
[11] A. Keresztessy, I. P. Nagy, Gy. Bazsa, and J. A. Pojman, J. Phys. Chem. **99**, 5379 (1995).
[12] M. Böckmann and S. C. Müller, Phys. Rev. Lett. **85**, 2506 (2000).
[13] D. Horváth, T. Bánsági, Jr., and Á. Tóth, J. Chem. Phys. **117**, 4399 (2002).
[14] J. Huang, D. A. Vasquez, B. F. Edwards, and P. Kolodner, Phys. Rev. E **48**, 4378 (1993).
[15] A. De Wit, Phys. Rev. Lett. **87**, 054502 (2001).
[16] J. Martin, N. Rakotomalala, D. Salin, and M. Böckmann, Phys. Rev. E **65**, 051605 (2002).
[17] A. De Wit and G. M. Homsy, J. Chem. Phys. **107**, 9609 (1997); **107**, 9619 (1997).
[18] L. Szirovicza, I. Nagypál, and E. Boga, J. Am. Chem. Soc. **111**, 2842 (1989).
[19] Á. Tóth, I. Lagzi, and D. Horváth, J. Phys. Chem. **100**, 14 837 (1996).
[20] D. Horváth and Á. Tóth, J. Chem. Phys. **108**, 1447 (1998).
[21] F. Gauffre, V. Labrot, J. Boissonade, P. De Kepper, and E. Dulos, J. Phys. Chem. A **107**, 4452 (2003).
[22] I. Szalai, F. Gauffre, V. Labrot, J. Boissonade, and P. De Kepper, J. Phys. Chem. A **109**, 7843 (2005).
[23] T. Bánsági, Jr., D. Horváth, and Á. Tóth, Phys. Rev. E **68**, 026303 (2003).
[24] T. Bánsági, Jr., D. Horváth, and Á. Tóth, Chem. Phys. Lett. **384**, 153 (2004).
[25] J. Yang, A. D'Onofrio, S. Kalliadasis, and A. De Wit, J. Chem. Phys. **117**, 9395 (2002).
[26] D. A. Vasquez and A. De Wit, J. Chem. Phys. **121**, 935 (2004).
[27] D. Lima, A. D'Onofrio, and A. De Wit, J. Chem. Phys. **124**, 014509 (2006).
[28] Chemical composition of the reactant mixture: $[K_2S_4O_6]_0 = 2.5$–6.25 mM, $[NaClO_2]_0 = 10.0$–25.0 mM, $[NaOH]_0 = 1.0$–10.0 mM, and the Congored indicator in 0.4 mg/cm^3.
[29] B. Benjumea, J. A. Hunter, J. M. Aylsworth, and S. E. Pullan, Tectonophysics **368**, 193 (2003).
[30] E. W. Hudson, R. W. Simmonds, C. A. Y. Leon, S. H. Pan, and J. C. Davis, Czech. J. Phys. **46**, 2737 (1996).
[31] A. Jaree, R. R. Hudgins, H. Budman, P. L. Silveston, V. Yakhnin, and M. Menzinger, Chem. Eng. Sci. **58**, 833 (2003).
[32] M. L. Andermann, J. Ritt, M. A. Neimark, and C. I. Moore, Neuron **42**, 451 (2004).